Asian Spine Journal
Clinical Study
Asian Spine J 2024;18(2):209-217 • https://doi.org/10.31616/asj.2023.0339

Sagittal Section Hounsfield Units of the Upper Instrumented Vertebrae as a Predictor of Proximal Junctional Vertebral Fractures Following Adult Spinal Deformity Surgery

Koichi Murata[1], Bungo Otsuki[1], Takayoshi Shimizu[1], Takashi Sono[1], Shunsuke Fujibayashi[1,2], Shuichi Matsuda[1]

[1]*Department of Orthopaedic Surgery, Kyoto University Graduate School of Medicine, Kyoto, Japan*
[2]*Department of Orthopaedic Surgery, Kijunkai Yoshikawa Hospital, Kyoto, Japan*

Study Design: A retrospective observational study.

Purpose: This study aimed to determine an accurate and convenient screening method for predicting proximal junctional fractures (PJFr) following surgery for adult spinal deformity (ASD) using computed tomography (CT)-based measurement of Hounsfield units (HUs).

Overview of Literature: CT-based measurement of HUs is an alternative tool for assessing bone mineral density. However, the optimal method for predicting adjacent vertebral fractures following spinal fusion using HUs remains unclear.

Methods: This retrospective observational study included 42 patients who underwent reconstructive surgery for ASD. Elliptical regions of interest (ROIs) on the axial section and rectangular ROIs on the sagittal section were placed at the upper instrumented vertebrae (UIV), UIV+1, and UIV+2. In addition, the HU value of the L2 vertebra was used as the representative.

Results: PJFr occurred in 28.6% of patients within 2 years following surgery. The HU values obtained from the axial sections of L2, UIV, UIV+1, and UIV+2 were not significantly associated with the incidence of PJFr within 2 years, except for the ROI set in the lower region of the L2 vertebra. However, the HU value of the anterior third of the UIV in the sagittal section was significantly lower in the PJFr group than in the nonPJFr group (87.0 vs. 160.3, p=0.001). A UIV HU value of <100 was associated with a higher incidence of PJFr than an HU vaue of >100 (p<0.05).

Conclusions: Measurements of HU in the anterior one-third of the UIV in the sagittal section demonstrated predictive ability for PJFr following ASD surgery. A UIV HU value of <100 emerged as a risk factor for PJFr.

Keywords: Bone mineral density; Computed X-ray tomography; Osteoporosis; Spondylosis; Adult spinal deformity

Introduction

Symptomatic proximal junctional kyphosis (PJK), also referred to as proximal junctional failure, may require additional surgical intervention following corrective surgery for adult spinal deformity (ASD) [1]. Proximal junctional

Received Oct 16, 2023; Revised Dec 13, 2023; Accepted Dec 21, 2023
Corresponding author: Koichi Murata
Department of Orthopaedic Surgery, Kyoto University Graduate School of Medicine, 54 Kawahara-cho, Shogoin, Sakyo, Kyoto, 606-8507, Japan
Tel: +81-75-751-3877, Fax: +81-75-751-3885, E-mail: kchm@kuhp.kyoto-u.ac.jp

fractures (PJFr) are the most common cause of PJK and have been observed in approximately 51% of patients with PJK [2]. Risk factors for PJFr include high body mass index, advanced age, presence of osteoporosis, choice of the upper instrumented vertebra (UIV), and spinopelvic parameters [3]. Among these risk factors, low bone mineral density (BMD) and osteoporosis are considered significant contributors.

Currently, dual-energy X-ray absorptiometry (DEXA) is the gold standard for assessing BMD and diagnosing osteoporosis [4]. However, DEXA may yield inaccurate results in the diagnosis of osteoporosis. Factors such as sclerotic lesions, scoliosis, spinal degeneration, vertebral fractures, and abdominal aortic calcification can lead to an overestimation of BMD when assessed using DEXA.

Recently, there have been suggestions to use computed tomography (CT) and analyze Hounsfield unit (HU) measurements as supplementary methods for assessing BMD. Unlike DEXA, CT is not affected by measurement errors caused by degenerative changes, and a positive correlation between CT HU values and DEXA BMD was established [4]. HU measurements are also correlated with future osteoporotic fracture risk, cage subsidence following interbody fusion, pedicle screw loosening, and symptomatic pseudarthrosis following posterolateral fusion [5-10]. Considering these findings, spine experts recommended that patients aged ≥65 years, as well as those aged <65 years with specific risk factors, should undergo a comprehensive bone health assessment that includes CT-based measurement of the HU value [11,12].

The association of HU with the development of PJK or mechanical complications has been suggested [13-17]. However, the optimal method for measuring HU values to predict postoperative PJFr remains unknown. Thus, whether the use of the HU value of the UIV or representative HU of vertebral bodies in the lumbar spine, such as L2, like in DEXA, is more accurate remains unclear. This study aimed to analyze HU values in different vertebrae and regions of interest (ROI) within thoracolumbar CT images to propose a more precise and convenient screening method for predicting PJFr following ASD surgery.

Materials and Methods

1. Patients

From January 2013 to August 2019, 120 patients aged >50 years who underwent spinal fusion and were diagnosed with ASD were reviewed. ASD was defined as the presence of at least one of the following: sagittal vertical axis (SVA) >50 mm, coronal Cobb angle >20°, pelvic tilt (PT) >25°, or thoracic kyphosis (TK) >60° [18,19]. Patients who underwent instrumentation from the UIV between T7 and L2, along with sacral fusion of the lowest instrumented vertebrae, with or without iliac fixation, were enrolled. Patients were required to have a minimum follow-up of 2 years. Patients with a history of two lumbar spine surgeries were excluded (Fig. 1).

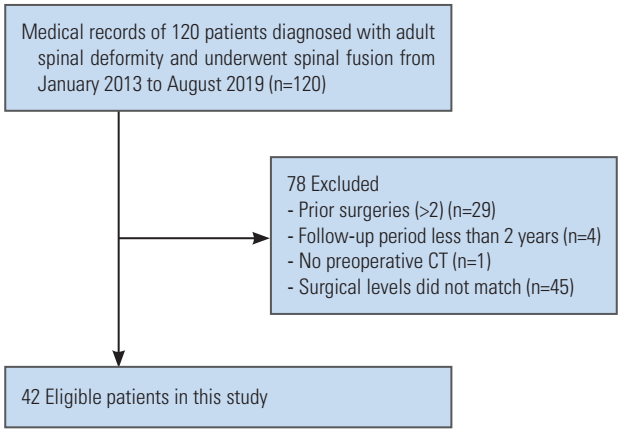

Fig. 1. Study flow chart. CT, computed tomography.

This study was approved by the ethics committee of the authors' affiliated institutions and was conducted in compliance with the principles of the Declaration of Helsinki. Informed consent was waived because of the retrospective design.

2. Radiographic assessment

Lateral spine radiographs were obtained at baseline (before surgery), 3 and 6 months after surgery, and annually thereafter until the final follow-up. These radiographs were used to evaluate morphometric vertebral fractures. To determine the anterior, posterior, and mid-height, six points were marked on each vertebra. PJFr were defined as new fractures occurring at the UIV, UIV+1, or UIV+2 levels, with a reduction in vertebral height of >20% (minimum of 4 mm) from baseline measurements [20]. Acute vertebral fractures were determined using magnetic resonance imaging, which showed characteristic patterns of low-intensity signal changes on T1-weighted images and high-intensity signal changes on T2-weighted images [21].

In this study, various radiographic parameters were

assessed, including PT, lumbar lordosis (LL) from L1 to S1, pelvic incidence (PI), TK between T4 and T12, SVA, LL from L4 to S1, and global tilt [22]. The proximal junctional angle (PJA), UIV slope (angle between the superior endplate of the UIV and the horizontal plane), UIV inclination (angle between a line crossing the center of the vertebral body from UIV-2 to UIV and the vertical line), and UIV tilt (angle between a line parallel to the upper endplate of the upper instrumented vertebra and the horizontal line) were also measured [23-25]. Moreover, the occupancy rate of the pedicle screw was evaluated as previously outlined [26]. The angle of the UIV pedicle screw was determined by the orientation of the screw shaft relative to the superior vertebral endplate [27]. A screw was considered caudally directed if it was angled >2° downward from the superior endplate.

Furthermore, patients were categorized according to Roussouly's newly proposed classification for categorizing the progression of asymptomatic spinal typologies under degenerative conditions based on the SS and LL contours [28]. Patients were also grouped according to the degree of LL correction relative to PI by adjusting for age, which uses the following formula [29,30]: (age-adjusted ideal PI–LL)–(postoperative PI–LL). The three groups were as follows: group U (undercorrection; <10°), group I (ideal correction; −10° to 10°), and group O (overcorrection; >10°). Following the calculation of the five components of the Global Alignment and Proportion (GAP) score, patients were further classified into proportionate, moderately disproportionate, and severely disproportionate groups [22].

3. Computed tomography assessment

CT was performed using different multidetector scanners (Siemens SOMATOM Sensation Open [Siemens Healthineers AG, Forchheim, Germany], Canon Medical Aquilion PRIME [Canon Medical System Corp., Tochigi, Japan], Philips Ingenuity Core 64 slice [Philips, Amsterdam, The Netherlands]) with a consistent peak voltage of 120 kV and variable protocol-specific tube current (mA) settings. Although the kV settings strongly affected the HU values of the bone, the mA settings only influenced the noise levels [31].

To assess osteoporosis and bone fragility using the HU values of the vertebral body, different methods for ROI selection were employed. ROIs are typically set on an axial slice of the L2 vertebral body. Because HU values varied

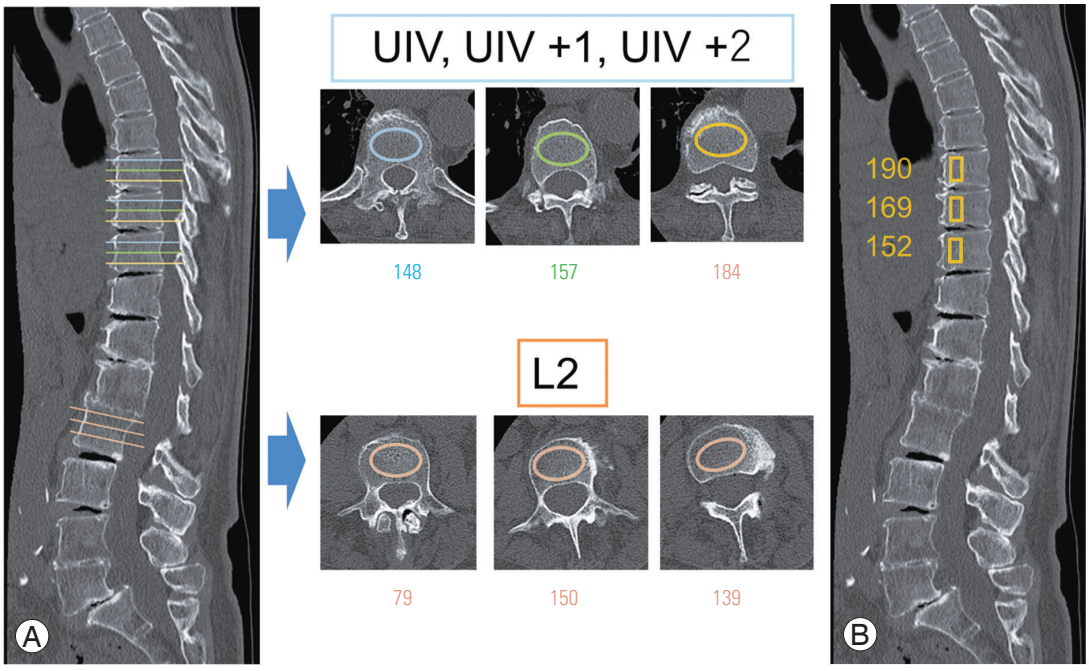

Fig. 2. Demonstration of Hounsfield unit (HU) measurement. **(A)** HU value in axial plane. HU values of upper instrumented vertebra (UIV), UIV+1, UIV+2, and L2 were measured in axial plane, by placing the elliptical regions of interests (ROIs) at the upper 1/3 level, the middle, and lower 1/3 levels. **(B)** The HU value of the anterior 1/3 of the vertebral body was measured in the midsagittal plane by manually placing rectangle ROIs.

across different heights within the same vertebral body, elliptical ROIs were placed on the upper, middle, and lower thirds of the vertebral body to measure HU values. The HU values were also measured at the UIV, UIV+1, and UIV+2 levels. The average and lowest values were calculated, and their relationship with the incidence of PJFr within 2 years was investigated.

The HU values of the anterior third of the vertebral body (UIV, UIV+1, and UIV+2) were also measured in the median and adjacent left and right planes on sagittal CT images. A rectangular ROI was manually placed, and the lowest HU value of the vertebral body was selected while avoiding areas with cortical bone or severe sclerotic abnormalities (Fig. 2) [10].

4. Statistical analyses

Statistical analyses were performed using JMP Pro ver. 15.0 (SAS Institute Inc., Cary, NC, USA) or R ver. 4.3.2 (The R Foundation for Statistical Computing, Vienna, Austria) with a two-tailed paired *t*-test (two conditions). Kaplan-Meier plots were used to illustrate fracture-free survival for the participants according to their HU values. The log-rank test was used to evaluate the statistical significance of the differences between the groups. The time to PJFr was analyzed using multivariate Cox proportional hazards modeling. Statistical significance was set at $p<0.05$.

Results

The study included 42 patients with a mean age of 69.2±9.1 years. Overall, 83.3% of the patients were female, and 23.8% had a history of lumbar surgery. The UIV levels were distributed as follows: L2, T10, and T9. Iliac fixation was performed in 76.2% of the patients. The characteristics of the participants are provided in Table 1.

Twelve patients experienced PJFr within 2 years following surgery. No significant differences in age, sex, history of previous surgery, UIV level, history of lumbar surgery, or body mass index were found between the PJFr and nonPJFr groups. Pre- and postoperative radiographic parameters are shown in Table 2. No statistically significant differences were found in the preoperative LL, PI, PI–LL, PT, SVA, or global tilt between the PJFr and nonPJFr groups. No significant differences in Roussouly classification, GAP classification, PJA, UIV tilt angle, UIV slope, or UIV inclination were noted between the two groups. Similarly, no significant differences in postoperative LL, PT, PI–LL, age-adjusted PI–LL, SVA, global tilt, or screw occupancy ratio were found between the two groups. The proportion of the caudally directed screws was significantly higher in the PJFr group than in the nonPJFr group ($p<0.01$).

Table 1. Patients' characteristics

Characteristic	All (n=42)	PJFr (n=12)	No PJFr (n=30)	*p*-value
No. of female	35 (83.3)	11 (91.7)	24 (80.0)	0.65
Age (yr)	69.2±9.1	72.8±6.8	67.7±9.6	0.06
Body mass index (kg/m^2)	22.8±3.3	22.9	24.1	0.26
Prior surgery				
0	32	9	23	1
1	10	3	7	
UIV				
T7	3	1	2	NA
T8	3	0	3	
T9	7	3	4	
T10	12	4	8	
L1	1	0	1	
L2	16	4	12	
LIV				
S	4	2	2	0.56
I	38	10	28	
UIV construct				
Pedicle screw	36	10	26	0.61
Pedicle screw and hook	5	2	3	
Hook	1	0	1	
Pedicle subtraction osteotomy	10 (23.8)	2 (16.7)	8 (26.7)	0.7
Operation time (min)	439±123	434±95	441±136	0.86
Estimated blood loss (mL)	773±932	860.9±713.2	734.4±1,025.1	0.67

Values are presented as number (%), mean±standard deviation, or number.
PJFr, proximal junctional fractures; UIV, upper instrumented vertebra; LIV, lower instrumented vertebra.

The ROI was set on the axial plane of L2 as a representative. HU values in the axial plane differed depending on the vertebral body level. In the lower slice, the L2 HU values were significantly lower in the PJFr group than in the nonPJFr group ($p=0.01$). However, no significant differences were observed in the other ROIs (Table 3).

Furthermore, ROIs were set in the axial plane of the UIV. Elliptical ROIs were placed on the upper, middle,

Table 2. Comparison of preoperative and postoperative radiographic indices

Variable	PJFr (n=12)	No PJFr (n=30)	*p*-value
Preoperative parameters			
PI (°)	45.3±8.1	50.3±14.8	0.18
PT (°)	35.5±8.8	34.3±13.6	0.73
LL (°)	-3.6±16.3	6.6±16.7	0.08
PI–LL (°)	49.0±18.0	43.6±20.3	0.41
SVA (mm)	128.2±50.6	107.3±60.0	0.26
Global tilt (°)	26.3±12.7	23.7±9.2	0.53
PJA (°)	3.1±10.6	5.3±7.5	0.51
Roussouly Classification			0.32
Type 1	0 (0)	4 (13.3)	
Retroverted type 2+TK	0 (0)	1 (3.3)	
Global kyphosis	12 (100)	25 (83.3)	
UIV tilt angle (°)	2.4±5.0	0.4±5.0	0.24
UIV slope (°)	3.5±9.6	3.2±10.1	0.93
UIV inclination (°)	15.1±4.2	13.9±9.0	0.55
GAP score	9.7±3.7	7.8±2.5	0.06
GAP classification			0.56
Proportionated (1–2)	0 (0)	1 (3.3)	
Moderately disproportionated (3–6)	4 (33.3)	6 (20.0)	
Severely disproportionated (7–13)	8 (66.7)	23 (76.7)	
Postoperative parameters			
PT (°)	23.7±8.3	23.3±8.2	0.9
LL (°)	32.5±15.0	34.8±12.7	0.66
PI–LL (°)	12.5±12.4	12.6±15.2	0.98
SVA (mm)	31.6±39.5	26.6±44.6	0.72
Global tilt (°)	26.3±12.7	23.7±9.2	0.53
Age-adjusted PI–LL			0.63
Under correct	4 (33.3)	7 (23.3)	
Normal	3 (25.0)	12 (40.0)	
Overcorrect	5 (41.7)	11 (36.7)	
Caudal directed screw (UIV)	8 (66.7)	7 (24.1)	0.01
UIV screw occupancy ratio (%)	60.8±17.8	60.5±13.2	0.95
UIV screw occupancy ratio >80%	1 (8.3)	2 (6.7)	0.85

Values are presented as mean±standard deviation or number (%).
PJFr, proximal junctional fracture; PI, pelvic incidence; PT, pelvic tilt; LL, lumbar lordosis; SVA, sagittal vertical axis; PJA, proximal junctional angle; TK, thoracic kyphosis; UIV, uppermost instrumented vertebra; GAP score, Global Alignment and Proportion score.

and lower thirds of the vertebral body, and the minimum and average HU values were calculated. No statistical difference was found in the HU values between the PJFr and nonPJFr groups (Table 3). In addition, the average or minimum HU values of the axial slice in the UIV did not differ between the PJFr and nonPJFr groups. When the ROI was set in the axial plane of UIV+1 or UIV+2, the HU values in each section were not significantly different. No differences were observed in the average or minimum HU values in the axial section of UIV+1 and UIV+2.

Table 3. Comparison of Hounsfield unit values between patients with and those without proximal junctional fracture

Variable	PJFr (n=12)	No PJFr (n=30)	*p*-value
L2 (axial, upper)	104.8±47.5	132.0±61.0	0.14
L2 (axial, middle)	108.4±41.2	127.0±65.4	0.28
L2 (axial, lower)	113.4±42.9	168.4±98.2	0.01
L2 (axial, average)	108.9±41.1	142.5±68.3	0.05
L2 (axial, min)	93.7±37.2	113.2±54.1	0.19
UIV (axial, upper)	114.8±49.9	142.4±43.2	0.11
UIV (axial, middle)	127.3±42.3	150.7±68.0	0.19
UIV (axial, lower)	126.7±50.9	162.4±92.9	0.12
UIV+1 (axial, upper)	115.4±40.1	125.3±43.6	0.49
UIV+1(axial, middle)	127.5±35.7	141.6±40.8	0.28
UIV+1 (axial, lower)	126.2±37.8	136.3±39.2	0.45
UIV+2 (axial, upper)	137.8±82.1	141.8±50.9	0.88
UIV+2 (axial, middle)	137.0±32.0	146.5±45.4	0.46
UIV+2 (axial, lower)	138.6±47.8	137.2±43.9	0.93
UIV (axial, average)	122.9±44.8	151.8±60.4	0.1
UIV+1 (axial, average)	123.0±33.6	134.4±37.7	0.35
UIV+2 (axial, average)	137.8±52.1	141.8±43.5	0.82
UIV, UIV+1, UIV+2 (axial, upper, min)	100.5±41.4	117.7±37.9	0.23
UIV, UIV+1, UIV+2 (axial, middle, min)	112.9±35.9	129.5±37.8	0.2
UIV, UIV+1, UIV+2 (axial, lower, min)	110.8±36.0	124.2±38.0	0.29
UIV, UIV+1, UIV+2 (axial, all, min)	95.3±36.9	113.2±36.3	0.17
UIV (sagittal)	87.0±28.6	160.3±106.6	0.001
UIV, UIV+1, UIV+2 (sagittal, average)	78.8±30.7	110.9±39.3	0.004
UIV, UIV+1, UIV+2 (sagittal, min)	92.7±27.3	139.3±49.6	0.0004

Values are presented as mean±standard deviation.
PJFr, proximal junctional fracture; UIV, upper instrumented vertebra; min, minimum.

The HU value of the anterior third of the UIV was significantly lower in the PJFr group than in the nonPJFr group (Table 3). The mean or minimum HU values of the anterior one-third of the sagittal section of the UIV, UIV+1, and UIV+2 groups were significantly lower in the PJFr group than in the nonPJFr group.

Receiver operating characteristic curves were generated for the HU values in the sagittal plane of each patient to

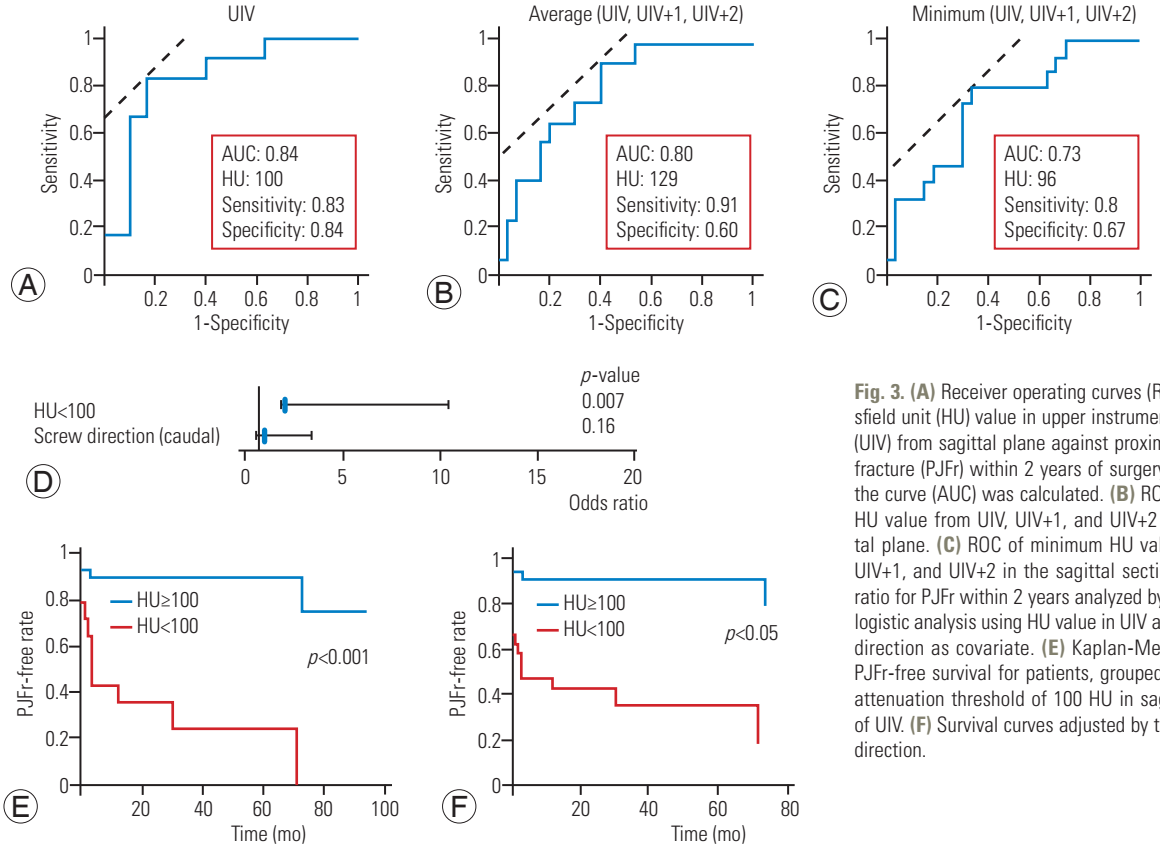

Fig. 3. **(A)** Receiver operating curves (ROC) of Hounsfield unit (HU) value in upper instrumented vertebra (UIV) from sagittal plane against proximal junctional fracture (PJFr) within 2 years of surgery. Area under the curve (AUC) was calculated. **(B)** ROC of average HU value from UIV, UIV+1, and UIV+2 in the sagittal plane. **(C)** ROC of minimum HU value from UIV, UIV+1, and UIV+2 in the sagittal section. **(D)** Odds ratio for PJFr within 2 years analyzed by multivariate logistic analysis using HU value in UIV and UIV screw direction as covariate. **(E)** Kaplan-Meier curves of PJFr-free survival for patients, grouped by vertebral attenuation threshold of 100 HU in sagittal section of UIV. **(F)** Survival curves adjusted by the UIV screw direction.

predict vertebral fractures within 2 years following surgery (Fig. 3A–C). The area under the curve was the largest in the order of UIV, mean HU value, and minimum HU value in the sagittal section. These findings suggest that the HU value of the UIV in the sagittal plane provides a more accurate prediction of future PJFr.

At a cutoff value of 100.1, the sensitivity and specificity were 1.0 and 0.39, respectively. Therefore, a cutoff value of 100 was chosen for this study. Regarding postoperative spinal parameters, a significant difference was observed in the direction of the UIV screw between the PJFr and nonPJFr groups (Table 2). Multivariate logistic regression analysis showed that a UIV HU value of <100 was a significant risk factor for the occurrence of PJFr within 2 years (Fig. 3D). Accordingly, patients with a UIV HU value of <100 experienced a higher incidence of PJFr than those with a value of >100 ($p<0.05$) (Fig. 3E), and the same result was obtained when the direction of the UIV screw was analyzed as a covariate (Fig. 3F).

Discussion

In this study, HU values on sagittal images were more effective than those on vertebral axial images in predicting PJFr. Moreover, PJFr could be predicted by assessing the HU values of the UIV alone, without measuring UIV, UIV+1, and UIV+2.

Assessing bone quality before surgical correction of ASD is crucial because of the potential complications associated with PJFr in both the patients and treatment team. DEXA is considered the gold standard for BMD assessment. However, DEXA is not optimal for assessing BMD in the presence of degenerative changes or spinal deformities. In addition, DEXA is not specifically designed for ASD surgery in terms of measurement sites and thresholds because the thoracic spine is not a standard area for DEXA. However, HU values can be used to estimate regional bone strength. For example, the HU value of the screw trajectory can be measured, and the cortical bone trajectory was found to have significantly higher CT values than the conventional pedicle screw trajectory [32]. Another study demonstrated a correlation between HU values and pedicle screw insertion torque [33]. Similarly, CT-based HU values can directly evaluate the BMD of the anterior portion of the UIV, which is susceptible to collapse.

The present study set a rectangular ROI in the anterior

one-third of the vertebral body, whereas previous studies often used an elliptical ROI encompassing the entire vertebral body. Studies have reported spatial heterogeneity in the trabecular bone density within the vertebra [34-36]. To minimize vertebral heterogeneity, recent reports evaluating the risk of proximal junctional failure adopted a method to calculate the average HU values by setting the elliptical ROI immediately inferior to the superior end plate, middle of the vertebral body, and superior to the inferior endplate [13-15,17]. Wedge fractures can be associated with low BMD in the superior anterior region [37]. Therefore, evaluating the HU value in the anterior one-third of the vertebral body is reasonable, although few studies have demonstrated the usefulness of HU values measured in the anterior third of the sagittal plane compared with those in the axial plane [10]. In this study, we could not find a difference in the averaged HU value of UIV, UIV+1, or UIV+2. Given the small number of cases in this study, the average HU value of the axial section may not have shown a statistically significant difference. However, measuring the HU value at the sagittal section may be more sensitive to predict PJFr.

In this study, DEXA-derived BMD data were unavailable. Previous studies have focused on the lumbar spine and established thresholds, such as 135 HU for osteopenic spines, 120 HU for pedicle screw loosening, 110 HU for osteoporotic spines, and 90 HU for vertebral fracture [4,38,39]. Although these studies have evaluated HU values using axial slices, our cutoff level of 100 was similar to that of previous reports.

Previously, we reported that each vertebral body had different HU values in the sagittal plane depending on the level [10]. Furthermore, lower HU thresholds are associated with higher specificity and lower sensitivity for detecting osteoporosis and predicting fractures, whereas higher thresholds are associated with lower specificity and higher sensitivity. In addition, the optimal thresholds for estimating the PJFr risk using the HU values of representative vertebral bodies may differ from those for predicting the PJFr risk in individual vertebrae, considering the spinal alignment, fixed levels, and fragile sites within the vertebral bodies. Optimal thresholds for each application must be proposed.

This study has some limitations. First, BMD was not measured using DEXA, as previously mentioned, and the corresponding BMD values for specific HU values remain unknown. Second, the relationship between the effects of osteoporotic drugs and HU values was not investigated. Further studies are needed to assess the preventive effects of antiosteoporotic drugs, braces, and changes in surgical strategies, which may influence HU values. Third, the number of patients was limited. PJFr has multifactorial causes and is affected by various factors, including preoperative and postoperative spinal parameters and their changes, UIV fixation method, osteoporosis, and other factors. In this study, no difference in spinal parameters was noted between the PJFr and nonPJFr groups, and the contribution of each risk factor to PJFr could not be compared.

Conclusions

CT-based measurement of the HU value in the anterior one-third of the vertebral body was predictive of the PJFr risk following ASD surgery. The HU values obtained from the sagittal images more effectively predict PJFr than the values obtained from the axial images. Specifically, a UIV HU value of <100 was identified as a significant risk factor for PJFr.

Conflict of Interest

No potential conflict of interest relevant to this article was reported.

ORCID

Koichi Murata: https://orcid.org/0000-0002-7896-3937; Bungo Otsuki: https://orcid.org/0000-0002-4749-7830; Takayoshi Shimizu: https://orcid.org/0000-0002-2683-0489; Takashi Sono: https://orcid.org/0000-0001-5599-0185; Shunsuke Fujibayashi: https://orcid.org/0000-0003-0662-4298; Shuichi Matsuda: https://orcid.org/0000-0003-0802-1255

Author Contributions

Conceptualization: Koichi Murata. Methodology: Koichi Murata. Data curation: Koichi Murata. Investigation: Bungo Otsuki, Takayoshi Shimizu, Takashi Sono, Shunsuke Fujibayashi. Writing–original draft: Koichi Murata. Writing–review & editing: Bungo Otsuki, Takayoshi Shimizu, Takashi Sono, Shunsuke Fujibayashi, Shuichi Matsuda. Supervision: Shuichi Matsuda. Final approval of the manuscript: all authors.

References

1. Patel SA, McDonald CL, Reid DB, DiSilvestro KJ, Daniels AH, Rihn JA. Complications of thoracolumbar adult spinal deformity surgery. JBJS Rev 2020;8:e0214.
2. Maruo K, Ha Y, Inoue S, et al. Predictive factors for proximal junctional kyphosis in long fusions to the sacrum in adult spinal deformity. Spine (Phila Pa 1976) 2013;38:E1469-76.
3. Sardar ZM, Kim Y, Lafage V, et al. State of the art: proximal junctional kyphosis-diagnosis, management and prevention. Spine Deform 2021;9:635-44.
4. Zaidi Q, Danisa OA, Cheng W. Measurement techniques and utility of hounsfield unit values for assessment of bone quality prior to spinal instrumentation: a review of current literature. Spine (Phila Pa 1976) 2019;44:E239-44.
5. Nguyen HS, Shabani S, Patel M, Maiman D. Posterolateral lumbar fusion: relationship between computed tomography Hounsfield units and symptomatic pseudoarthrosis. Surg Neurol Int 2015;6(Suppl 24):S611-4.
6. Matsukawa K, Abe Y, Yanai Y, Yato Y. Regional Hounsfield unit measurement of screw trajectory for predicting pedicle screw fixation using cortical bone trajectory: a retrospective cohort study. Acta Neurochir (Wien) 2018;160:405-11.
7. Zou D, Muheremu A, Sun Z, Zhong W, Jiang S, Li W. Computed tomography Hounsfield unit-based prediction of pedicle screw loosening after surgery for degenerative lumbar spine disease. J Neurosurg Spine 2020;32:716-21.
8. Bredow J, Boese CK, Werner CM, et al. Predictive validity of preoperative CT scans and the risk of pedicle screw loosening in spinal surgery. Arch Orthop Trauma Surg 2016;136:1063-7.
9. Mi J, Li K, Zhao X, Zhao CQ, Li H, Zhao J. Vertebral body Hounsfield units are associated with cage subsidence after transforaminal lumbar interbody fusion with unilateral pedicle screw fixation. Clin Spine Surg 2017;30:E1130-6.
10. Murata K, Fujibayashi S, Otsuki B, Shimizu T, Matsuda S. Low Hounsfield unit values at sagittal section on computed tomography predicts vertebral fracture following short spinal fusion. J Orthop Sci 2023 Mar 21 [Epub]. https://doi.org/10.1016/j.jos.2023.03.008
11. Dimar J, Bisson EF, Dhall S, et al. Congress of Neurological Surgeons systematic review and evidence-based guidelines for perioperative spine: preoperative osteoporosis assessment. Neurosurgery 2021;89(Suppl 1):S19-25.
12. Sardar ZM, Coury JR, Cerpa M, et al. Best practice guidelines for assessment and management of osteoporosis in adult patients undergoing elective spinal reconstruction. Spine (Phila Pa 1976) 2022;47:128-35.
13. Chanbour H, Chen JW, Vaughan WE, et al. Which bone mineral density measure offers a more reliable prediction of mechanical complications in adult spinal deformity surgery: Hounsfield units or DEXA scan? World Neurosurg 2023;178:e657-65.
14. Chanbour H, Steinle AM, Chen JW, et al. The importance of Hounsfield units in adult spinal deformity surgery: finding an optimal threshold to minimize the risk of mechanical complications. J Spine Surg 2023;9:149-58.
15. Hiyama A, Sakai D, Katoh H, Sato M, Watanabe M. Relationship between Hounsfield units of upper instrumented vertebrae, proximal junctional failure, and global alignment and proportion score in female patients with adult spinal deformity. World Neurosurg 2022;164:e706-17.
16. Duan PG, Mummaneni PV, Rivera J, et al. The association between lower Hounsfield units of the upper instrumented vertebra and proximal junctional kyphosis in adult spinal deformity surgery with a minimum 2-year follow-up. Neurosurg Focus 2020;49:E7.
17. Yoshie N, Maruo K, Arizumi F, Kishima K, Kusukawa T, Tachibana T. The relationship between the Hounsfield units value of the upper instrumented vertebra and the severity of proximal junctional fracture after adult spinal deformity surgery. Medicina (Kaunas) 2023;59:1086.
18. Terran J, Schwab F, Shaffrey CI, et al. The SRS-Schwab adult spinal deformity classification: assessment and clinical correlations based on a prospective operative and nonoperative cohort. Neurosurgery 2013;73:559-68.
19. Yasuda T, Hasegawa T, Yamato Y, et al. Postoperative change of thoracic kyphosis after corrective surgery for adult spinal deformity. Spine Surg Relat Res 2018;2:283-9.
20. Kurra S, Farhadi HF, Metkar U, et al. CT based bone mineral density as a predictor of proximal junctional fractures. N Am Spine Soc J 2022;11:100130.

21. Takahashi S, Hoshino M, Takayama K, et al. Predicting delayed union in osteoporotic vertebral fractures with consecutive magnetic resonance imaging in the acute phase: a multicenter cohort study. Osteoporos Int 2016;27:3567-75.
22. Yilgor C, Sogunmez N, Boissiere L, et al. Global Alignment and Proportion (GAP) Score: development and validation of a new method of analyzing spinopelvic alignment to predict mechanical complications after adult spinal deformity surgery. J Bone Joint Surg Am 2017;99:1661-72.
23. Im SK, Lee KY, Lee JH. The impact of upper instrumented vertebra orientation on proximal junctional kyphosis: a novel and fixed parameter, fused spinopelvic angle. Spine (Phila Pa 1976) 2022;47:1651-8.
24. Lafage R, Line BG, Gupta S, et al. Orientation of the upper-most instrumented segment influences proximal junctional disease following adult spinal deformity surgery. Spine (Phila Pa 1976) 2017;42:1570-7.
25. Chan CY, Chiu CK, Ler XY, et al. Upper instrumented vertebrae (UIV) tilt angle is an important postoperative radiological parameter that correlates with postoperative neck and medial shoulder imbalance. Spine (Phila Pa 1976) 2018;43:E1143-51.
26. Oe S, Yamato Y, Hasegawa T, et al. Occupancy rate of pedicle screw below 80% is a risk factor for upper instrumented vertebral fracture after adult spinal deformity surgery. Spine (Phila Pa 1976) 2023;48:843-52.
27. Chen JW, Longo M, Chanbour H, et al. Cranially directed upper instrumented vertebrae screw angles are associated with proximal junctional kyphosis in adult spinal deformity surgery. Spine (Phila Pa 1976) 2023;48:710-9.
28. Sebaaly A, Gehrchen M, Silvestre C, et al. Mechanical complications in adult spinal deformity and the effect of restoring the spinal shapes according to the Rousouly classification: a multicentric study. Eur Spine J 2020;29:904-13.
29. Park SJ, Lee CS, Kang BJ, et al. Validation of age-adjusted ideal sagittal alignment in terms of proximal junctional failure and clinical outcomes in adult spinal deformity. Spine (Phila Pa 1976) 2022;47:1737-45.
30. Byun CW, Cho JH, Lee CS, Lee DH, Hwang CJ. Effect of overcorrection on proximal junctional kyphosis in adult spinal deformity: analysis by age-adjusted ideal sagittal alignment. Spine J 2022;22:635-45.
31. Lee SJ, Graffy PM, Zea RD, Ziemlewicz TJ, Pickhardt PJ. Future osteoporotic fracture risk related to lumbar vertebral trabecular attenuation measured at routine body CT. J Bone Miner Res 2018;33:860-7.
32. Zhang RJ, Li HM, Gao H, Jia CY, Xing T, Shen CL. Associations between the Hounsfield unit values of different trajectories and bone mineral density of vertebrae: cortical bone and traditional trajectories. Am J Transl Res 2020;12:3906-16.
33. Ishikawa K, Toyone T, Shirahata T, et al. A novel method for the prediction of the pedicle screw stability: regional bone mineral density around the screw. Clin Spine Surg 2018;31:E473-80.
34. Kaiser J, Allaire B, Fein PM, et al. Heterogeneity and spatial distribution of intravertebral trabecular bone mineral density in the lumbar spine is associated with prevalent vertebral fracture. J Bone Miner Res 2020;35:641-8.
35. Hussein AI, Morgan EF. The effect of intravertebral heterogeneity in microstructure on vertebral strength and failure patterns. Osteoporos Int 2013;24:979-89.
36. Hussein AI, Jackman TM, Morgan SR, Barest GD, Morgan EF. The intravertebral distribution of bone density: correspondence to intervertebral disc health and implications for vertebral strength. Osteoporos Int 2013;24:3021-30.
37. Simpson EK, Parkinson IH, Manthey B, Fazzalari NL. Intervertebral disc disorganization is related to trabecular bone architecture in the lumbar spine. J Bone Miner Res 2001;16:681-7.
38. Anderson PA, Polly DW, Binkley NC, Pickhardt PJ. Clinical use of opportunistic computed tomography screening for osteoporosis. J Bone Joint Surg Am 2018;100:2073-81.
39. Deshpande N, Hadi MS, Lillard JC, et al. Alternatives to DEXA for the assessment of bone density: a systematic review of the literature and future recommendations. J Neurosurg Spine 2023;38:436-45.